

# On Determining and Qualifying the Number of Superstates in Aggregation of Markov Chains

Amber Srivastava, Raj K. Velicheti, and Srinivasa M. Salapaka

**Abstract**—A viable approach in the study of Markov chains with large state spaces is to determine a smaller representative chain that approximates the original stochastic model. Typically, the number of super-states in the aggregated Markov chain is pre-specified based on prior knowledge, computational limitations, or bounds on the representation error. In this paper we derive a quantity from the state-transition matrix of the original Markov chain that characterizes the reduction in the representation error for every additional super-state in the aggregated model. More precisely, we develop and quantify a notion of *persistence* for a given number of superstates, which captures the range of representation errors that the number of superstates can achieve. This quantity is justified using maximum entropy principle and studying sensitivity of representation errors with the number of superstates. Through simulations, we show that the number of superstates with the largest persistence detects the true number of superstates in synthetic datasets, where the true number is known a priori. This suggests of using the number of superstates with the largest persistence range as the target number of superstates.

## I. INTRODUCTION

Markov chains provide a stochastic model to study several real-world processes, such as population dynamics, cruise control, transportation systems, and queueing networks that are characterized by a sequence of stochastic events [1]. However, Markov chain models for several complex systems, such as applications originating in network analysis [2], neuroscience [3], and economics [4] require large number of states where simulating them is challenging and inefficient [5]; thus, laying foundation for several model reduction techniques in Markov chains [5]–[9].

A significant amount of work has been done in determining appropriate *dissimilarity* metrics [6]–[8] between a Markov chain and its representative aggregated model along with the algorithms that determine the latter for a pre-specified number of super-states such that the dissimilarity is minimized [8], [9]. However, there is scant literature that provides (a) guidance on the choice of number of super states, i.e., the number of aggregated states, and (b) a quantitative comparison between aggregated models obtained at different number of super-states; and thus, we seek to address them in our paper. Here, the additional challenge arises from the NP-hardness of the aggregation problem [10] which adds to the inherent complexities of (a) and (b). A recent work [11] partially addresses the above problems in the context of nearly completely decomposable (NCD) Markov chains wherein the proposed aggregation algorithm also provides an estimate for the number of super-states. However, in contrast to [11] we provide a method that compares the aggregated models of a given Markov chain with different number of

super-states, and demonstrate its utility in estimating the true number of super-states. A noticeable feature of our method is that we make it independent of the algorithm that obtains the aggregated models, thereby allowing a context-dependent aggregation algorithm instead of being restricted to a pre-specified algorithm.

We develop a quantity that measures the difference between the state transition matrices of the original and the aggregated Markov chains. More precisely, we view an  $N$ -state Markov chain as  $N$  points in an  $N$ -dimensional euclidean space, where  $k$ -th point represents the transition probability vector of the  $k$ -th state - that is, the  $k$ -th row in the state-transition matrix. We use concepts developed in [7], [9] to extend each probability row of the  $M$ -superstate Markov chain to an  $N$  dimensional vector thereby allowing comparison with the original Markov chain. Thereupon, we derive an *error covariance matrix* based on these probability vectors, the eigenvalues of which reflect the representation error between the original and the aggregated states - in terms of the differences between their respective transition probability vectors. This *error covariance matrix* has multiple applications. For instance, it qualifies each superstate; more precisely, it quantifies the *error spread* of each superstate, and therefore identifies which superstate needs to be *split* for maximum reduction in representation error.

Another important contribution of our work is the related notion of *persistence*. For a given set of aggregated models with different number  $k$  of superstates, we associate a *persistence* value to each  $k$ . More precisely, the persistence value of an aggregated model with  $k$  super-states is the ratio of largest eigenvalues of the error covariance matrices corresponding to model with  $k$  and  $k - 1$  superstates. The *persistence* reflects the range of representation errors that  $k$  superstates achieve in the given set of aggregated models. In fact, our simulations with many synthetic datasets, where *true* number of superstates are a priori known, demonstrate that the set of superstates with maximum persistence coincides with the number of true superstates.

Our work is motivated from the Markov chain aggregation framework presented in [9]. In particular, the solution methodology in [9] exhibits related quantities that derive our error covariance matrix and persistence. We substantiate further on this in the later sections. Below we define the error covariance matrix and persistence. Consider a Markov chain  $(X, \Pi)$  with state space  $X = \{x_i : 1 \leq i \leq N\}$ , and the transition probability matrix  $\Pi = (\pi_{ij}) \in \mathbb{R}^{N \times N}$ , its aggregated representative chain  $(Y, \Psi, \Phi)$  with state space  $Y = \{y_j : 1 \leq j \leq M\}$ , the transition probability matrix  $\Psi =$

$(\psi_{jk}) \in \mathbb{R}^{M \times M}$ , where  $M \ll N$ , and the associated partition function  $\Phi: X \rightarrow Y$  such that the state  $x_i \in X$  is covered by the super-state  $\Phi(x_i) \in Y$ .

**Definition 1.** The error covariance matrix associated to a super-state  $y_j \in Y$  that covers the states  $\Phi^{-1}(y_j) \subseteq X$  in the original Markov chain is given by

$$C_X^\Phi(y_j) := \sum_{x_i \in \Phi^{-1}(y_j)} \left[ \Theta^t \frac{(\pi(i) - w(j))}{w(j)} \right] \left[ \Theta^t \frac{(\pi(i) - w(j))}{w(j)} \right]^t, \quad (1)$$

where  $\pi(i) = (\pi_{i1}, \dots, \pi_{iN})$  denotes the transition probabilities of the state  $x_i$ ,  $w(j) := \frac{1}{|\Phi^{-1}(y_j)|} \sum_{x_i \in \Phi^{-1}(y_j)} \pi(i)$  denotes the association of the super-state  $y_j$  to each state in  $X$ ,  $\Theta \in \mathbb{R}^{N \times N-1}$  is illustrated in Appendix I,  $\frac{(\pi(i) - w(j))}{w(j)}$  denotes element-wise operation,  $[\cdot]^t$  denotes the transpose, and

$$RE(x_i, y_j) := \Theta^t \frac{(\pi(i) - w(j))}{w(j)} \quad (2)$$

in (1) denotes the representation error between  $x_i$  and  $y_j$ .

**Definition 2.** The persistence of  $k$  number of super-states in the  $K$  aggregated representations  $\{(Y_k, \Psi_k, \Phi_k) : |Y_k| = k\}_{k=1}^K$  of a Markov chain  $(X, \Pi)$  is given by

$$v(k) := \log \bar{T}_{k-1} - \log \bar{T}_k, \text{ where} \quad (3)$$

$$\bar{T}_l := \max_{1 \leq j \leq l} \left[ \lambda_{\max}(C_X^{\Phi_l}(y_j)) \right] \text{ for } l \in \{k-1, k\}, \quad (4)$$

and  $\lambda_{\max}(\cdot)$  denotes the largest eigenvalue.

The following proposition and the subsequent algorithm to compute persistence and estimate the true number  $k_t$  of super-states underlying a Markov chain  $(X, \Pi)$  summarizes the main contributions of our work.

**Proposition 1.** Given  $K$  aggregated representative chains  $\{(Y_k, \Psi_k, \Phi_k) : |Y_k| = k\}_{k=1}^K$  of a Markov chain  $(X, \Pi)$  the estimate  $k_t$  of the true number of super-states is given by

$$k_t := \arg \max_{1 \leq k \leq K} v(k), \quad (5)$$

where  $v(k)$  is the persistence of  $k$  super-states defined in (3).

---

#### Algorithm 1 Persistence and Number of Super-states

---

**Input:**  $\Pi, K$ ; **Output:**  $v(k), k_t$

**for**  $k = 1$  **to**  $K$  **do**

    aggregate  $\Pi$  and determine partition  $\Phi_k: X \rightarrow Y$ .

    compute  $w(j) = \frac{1}{|\Phi^{-1}(y_j)|} \sum_{x_i \in \Phi^{-1}(y_j)} \pi(i)$  and  $\bar{T}_k$  using (4).

**compute**  $v(k)$  in (3)  $\forall 2 \leq k \leq K$ , and  $k_t := \arg \max_k v(k)$ .

---

Our simulations demonstrate the efficacy of persistence in estimating the true number  $k_t$  of super-states. We observe that persistence value  $v(k_t)$  is as high as 50 to 400 times the second largest value for Markov chains where the true number  $k_t$  is discernible from the heatmap of the associated transition matrices  $\Pi$ . For Markov chains where true number  $k_t$  is not discernible from the heatmaps, i.e. the underlying true number  $k_t$  of super-states is not visually perceivable, the persistence value  $v(k_t)$  is still the largest and as high as 1.2 to 5 times the second largest value. This paper is

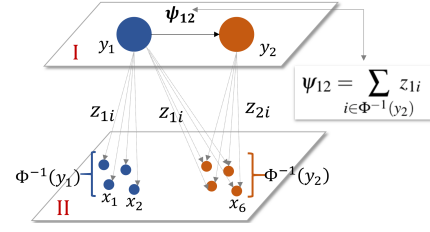


Fig. 1: The plane I represents the aggregated model for the Markov chain in the plane II. Each super-state  $y_j$  in I is associated to each state  $x_i$  in II via the weight  $z_{ji}$ . The set of states represented by super-state  $y_j$  is given by  $\Phi^{-1}(y_j)$ .

organized as follows. Section II summarizes the MEP-based aggregation framework in [9]. In Section III we provide an intuitive explanation for persistence and error covariance matrix, and relate them to the quantities obtained in the solution methodology of [9]. Section IV presents simulations.

## II. AGGREGATION OF A MARKOV CHAIN

In this section we briefly illustrate the model-reduction framework adopted in [9] that lays the foundation for the expression of error covariance matrix in (1) and the notion of persistence in (3). An essential component of determining the aggregated representation  $(Y, \Psi, \Phi)$  of a Markov chain  $(X, \Pi)$  is devising a mechanism to compare the two differently-sized stochastic models [6]–[9]. For instance, the framework in [9] associates an distribution vector  $z(j) = (z_{j1}, \dots, z_{jN}) \in \mathbb{R}^N$  to each super-state  $y_j \in Y$ , where  $\sum_{k=1}^N z_{jk} = 1$  and  $z_{jk} \geq 0$  for all  $k$ . Thereafter, it quantifies the distance  $d(x_i, y_j)$  between the state  $x_i$  and the super-state  $y_j$  as the relative entropy between the transition probability vector  $\pi(i) = (\pi_{i1}, \dots, \pi_{iN})$  of the state  $x_i$  and the distribution vector  $z(j)$ , where both  $\pi(i)$  and  $z(j)$  capture the relation of the state  $x_i$  and the super-state  $y_j$ , respectively, to all the  $N$  states in  $X$ . More precisely,

$$d(x_i, y_j) = \sum_{k=1}^N \pi_{ik} \log \frac{\pi_{ik}}{z_{jk}} \quad \forall \quad 1 \leq i \leq N, 1 \leq j \leq M. \quad (6)$$

Please refer to Figure 1 for a graphical interpretation of  $z(j)$ . The framework in [9] determines a set of  $M$  distribution vectors  $\{z(j)\}_{j=1}^M$  such that the cumulative distance of each state  $x_i$  to its closest super-state  $y_j := \Phi(x_i)$  (i.e., the super-state that represents  $x_i$ ) is minimized. In particular, [9] addresses the following optimization problem

$$\begin{aligned} \min_{Z, \Phi} \quad & D(\Pi, Z, \Phi) = \sum_{i=1}^N p_i d(x_i, \Phi(x_i)) \\ \text{subject to} \quad & z_{jk} \geq 0 \quad \forall j, k \text{ and } z(j)^t \mathbf{1}_N = 1 \quad \forall j, \end{aligned} \quad (7)$$

where  $p_i$  denotes the given relative weight of the state  $x_i$ . Subsequently, [9] determines the aggregated transition matrix  $\Psi = (\psi_{jk})$  in terms of the distribution vectors  $\{z(j)\}_{j=1}^M$ . In particular, the transition probability  $\psi_{jk}$  from the super-state  $y_j$  to  $y_k$  is the cumulative sum of the weights  $z_{ji}$ 's from super-state  $y_j$  to all states  $x_i$  that are represented by the super-state  $y_k$ , i.e.,  $x_i \in \Phi^{-1}(y_k)$  (see Figure 1), i.e.,  $\psi_{jk} = \sum_{x_i \in \Phi^{-1}(y_k)} z_{ji}$  for all  $1 \leq j, k \leq M$ .

The framework in [9] replaces the partition function  $\Phi(\cdot)$  by the soft association weights  $p_{ji} \in [0, 1]$  between all the states  $x_i$  and the super-states  $y_j$ , and uses Maximum Entropy Principle (MEP) to design the associations  $\{p_{ji}\}$ . In particular, [9] determines the most *unbiased* association weights  $P := \{p_{ji}\}$  and the distribution vectors  $\{z(j)\}$  that maximizes the corresponding Shannon entropy  $H$  such that the expected cost function  $\mathbb{E}_P[D]$  attains a pre-specified value  $d_0$ , that is, [9] solves the following optimization problem

$$\begin{aligned} \max_{P, \{z(j)\}} \quad & H = - \sum_{i=1}^N p_i \sum_{j=1}^M p_{ji} \log p_{ji} \\ \text{subject to} \quad & \mathbb{E}_P[D] := \sum_{i=1}^N p_i \sum_{j=1}^M p_{ji} d(x_i, y_j) = d_0 \\ & z_{jk} \geq 0, \quad z(j) \mathbf{1}_N = 1 \quad \forall j, k, \end{aligned} \quad (8)$$

repeatedly at decreasing values of  $d_0$  where the solution from the previous iteration is used to initialize the current iteration, and the algorithm terminates when the association weights become *hard*; that is  $p_{ji} \in \{0, 1\}$ . In the following section we develop an intuition for the notion of persistence.

### III. PERSISTENCE AND ITS QUANTIFICATION

#### A. Intuitive Description

The Markov chain aggregation problem in (7) can be re-interpreted as (a) partitioning (via the function  $\Phi: X \rightarrow Y$ ) a given set of  $N$  random variables  $\{\xi_i\}$  with distributions  $\{\pi(i)\}$  into  $M$  groups, and (b) determining a suitable representative distribution  $z(j)$  for each group such that the total relative entropy in (7) gets minimized; here, the relative entropy is interpreted as the *additional information* (or, additional number of bits) required, on average, to identify the random samples from the distributions  $\{\pi(i)\}$  using the optimal coding scheme constructed for the distribution  $z(\Phi(x_i))$ <sup>1</sup> [12]. This viewpoint enables us to relate the number of distinct representative distributions in  $\{z(j)\}$  to the amount of additional information  $d_0$  required to identify the samples from  $\{\pi(i)\}$ . In particular, for a pre-specified additional number of bits  $d_0$  in (8) there exists a *coarsest* representation that requires minimum number of distinct distributions in  $\{z(j)\}$ . For instance, at large values of  $d_0$  the optimization problem (8) results into a solution that comprises of *coincident* representative distributions in  $\{z(j)\}$ , and effectively  $M = 1$ , i.e., at large  $d_0$  it suffices to consider a single representative distribution to identify the samples from the distributions in  $\{\pi(i)\}$ . On the other hand, when the relative entropy  $d_0 = 0$ , the representative distribution  $z(\Phi(i))$  is *necessarily* same as  $\pi(i)$  for all  $1 \leq i \leq N$ , and the optimization problem (8) results into  $N$  *distinct* representative distributions in  $\{z(j)\}$ , and effectively  $M = N$ .

We adopt a graphical approach to illustrate the maximum variability (or, spread) in the representation error (2) for different scenarios of distinct number of distributions in

$\{z(j)\}$ ; where, the latter depends on the  $d_0$  values. Figure 2(a1) illustrates the heatmap of the state transition matrix  $\Pi$  of an NCD Markov chain with  $N = 27$  states. As illustrated by the heatmap,  $\Pi$  can either be considered to be composed of nine  $3 \times 3$  blocks (indicated by dark blue shade) or three  $9 \times 9$  blocks (indicated by a lighter blue shade) such that the states in the same block are more similar to each other than states in the other blocks. Figure 2(a2) provides a geometric interpretation of these 27 states where states  $x_{i_1}$  and  $x_{i_2}$  (equivalently the random variables  $\xi_{i_1}$  and  $\xi_{i_2}$ ) with transition probabilities  $\pi(i_1)$  and  $\pi(i_2)$  are placed spatially close to each other only if the relative-entropy  $d(x_{i_1}, x_{i_2})$  is small, otherwise  $x_{i_1}$  and  $x_{i_2}$  are kept spatially far. Alternatively, one can also think of each state  $x_i$  as an N-dimensional data point with coordinates  $\pi(i)$  where the spatial distance between  $x_{i_1}$  and  $x_{i_2}$  is the relative entropy  $d(x_{i_1}, x_{i_2})$ . Note that the three larger clusters containing 9 states denoted by  $\text{Clust}_L$  corresponds to the three  $9 \times 9$  blocks in  $\Pi$ , whereas the smaller clusters containing 3 states denoted by  $\text{Clust}_S$  correspond to  $3 \times 3$  blocks in  $\Pi$ .

Figure 2(a3) illustrates the maximum variability in the representation error observed at different number of distinct distributions in  $\{z(j)\}$ . For instance, the circle of radius  $r = \bar{T}_1$  denotes the maximum variability in the representation error (2) for a  $d_0$  value at which all distributions in  $\{z(j)\}$  are coincident, i.e. effectively  $M=1$ . The green annulus with outer radius  $r = \bar{T}_2$  and inner radius  $r = \bar{T}_3$  indicates the range  $[\bar{T}_3, \bar{T}_2]$  of maximum variability observed in the representation error (2) for the set of  $d_0$  values at which three distinct distributions in  $\{z(j)\}$  are required. Similarly, the blue annulus captures the range of maximum variability observed in the representation error when the set of  $d_0$  values require nine distinct distributions in  $\{z(j)\}$ .

We describe *persistence* of a given number  $k$  of super-states in terms of the range  $[\bar{T}_k, \bar{T}_{k-1}]$  of maximum variability (or, spread) observed in the representation error; where the spread  $\bar{T}_{k-1}$  (as quantified in the subsequent section) corresponds to the *largest* relative entropy  $d_0$  value at which  $k$  distinct distributions in  $\{z(j)\}$  are required, whereas the spread  $\bar{T}_k$  corresponds to the *smallest*  $d_0$  value at which  $k$  distinct distributions in  $\{z(j)\}$  suffice. In particular, we quantify persistence  $v(k)$  as in (3). We propose that the true number  $k_t$  of super-states in a Markov chain (analogously, true number  $k_t$  of representatives for  $\{\pi(i)\}$ ) is *characterized by the largest persistence, i.e., the largest range  $[\bar{T}_{k_t}, \bar{T}_{k_t-1}]$  of maximum variability in the representation error, i.e.,  $v(k_t) > v(k)$  for all  $k \neq k_t$ .*

We elucidate our quantification of persistence in (3) further by comparing the two distinct NCD Markov chains illustrated in Figure 2. As is evident from the heat maps in Figure 2(a1) and 2(b1) of the respective state transition matrices, the two Markov chains either comprise of three or nine super-states where three super-states is more dominant in Figure 2(a1) and nine super-states is more dominant in Figure 2(b1). This fact is appropriately captured in the Figures 2(a3) and 2(b3) by the large thicknesses of the green and blue annuluses corresponding to ranges  $[\bar{T}_3, \bar{T}_2]$

<sup>1</sup>Shannon Entropy  $H(q)$  quantifies the information required to identify samples from the distribution  $q$  when the latter is known. The relative entropy  $d(q, p)$  quantifies *additional* information required to identify samples from  $q$  using knowledge of the distribution  $p$  when  $q$  is unknown [12].

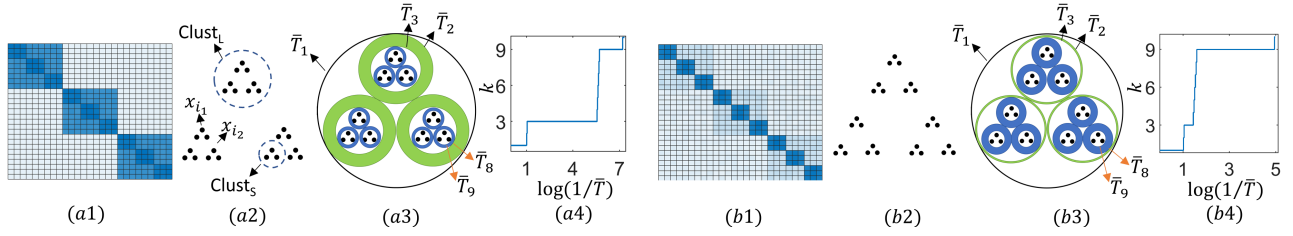


Fig. 2: Illustrates two  $N = 27$  NCD chains. (a1) Heatmap suggests 3 super-states dominates over 9. (a2) Geometric illustration (a3) Illustrates larger green annulus in comparison to blue annulus which implies 3 is the true number of super-states. (a4)  $k_t = 3$  persists for larger change in  $\log \frac{1}{\bar{T}}$  among all  $k$ . (b1)-(b4) Similar case where 9 super-states are dominant over 3.

and  $[\bar{T}_9, \bar{T}_8]$ , respectively. Additionally, Figures 2(a4) and 2(b4) plot the number  $k$  of distinct distributions in  $Z$  with respect to the range  $[\log(1/\bar{T}_{k-1}), \log(1/\bar{T}_k)]$  (scaled from  $[\bar{T}_k, \bar{T}_{k-1}]$  for better illustration). As can be seen from the plot, the range of  $\log(1/\bar{T})$  values for which either  $k = 3$  or  $k = 9$  distinct representative distributions in  $\{z(j)\}$  are observed is much larger than for any other  $k \notin \{3, 9\}$ . Further, the range of  $\log(1/\bar{T})$  is largest for  $k = 3$  in Figure 2(a4) and largest for  $k = 9$  in Figure 2(b4); thus, indicating that  $k_t = 3$  super-states in Figure 2(a1), whereas  $k_t = 9$  super-states in Figure 2(b1). This observation is in-line with the associated heatmaps. In the following section we motivate our expressions of the covariance matrix  $C_X^\Phi(\cdot)$  (1), the representation error  $RE(x_i, y_j)$  (2), and the corresponding spread  $\bar{T}_k$  (4) from analogous quantities that emanate in the solution methodology of [9].

### B. Quantitative Derivation of $\bar{T}_k$

Here we exploit the auxiliary cost function  $\mathcal{F}(Z)$  (also known as *free energy*) in [9] that results from minimizing the Lagrangian  $\mathcal{L} = (\mathbb{E}_P D - d_0) - TH$  of optimization problem in (8) with respect to association weights  $\{p_{j|i}\}$ , where  $T$  denotes the Lagrange parameter. The resulting free-energy

$$\mathcal{F}(Z) = -T \sum_{i=1}^N p_i \log \sum_{j=1}^M \exp \left\{ -\frac{1}{T} \sum_{k=1}^N \pi_{ik} \log \frac{\pi_{ik}}{z_{jk}} \right\}, \quad (9)$$

is a  $T$ -parameterized smooth log-sum-exp approximation of the expected cost function  $\mathbb{E}_P D$  in (8). Note that at large values of  $T (\rightarrow \infty)$  the Lagrangian  $\mathcal{L}$  is dominated by  $H$ , and free-energy  $\mathcal{F}(Z)$  is significantly different from the cost function  $\mathbb{E}_P D$ . As the parameter  $T \rightarrow 0$  the Lagrangian  $\mathcal{L}$  is dominated by  $\mathbb{E}_P D$ , and the free-energy  $\mathcal{F}(Z) \rightarrow \mathbb{E}_P D$ . Consequently, [9] exploits this homotopy from the convex function  $H$  to the non-convex  $\mathbb{E}_P D$  as  $T$  goes from a large value  $T_{\max} (\rightarrow \infty)$  to a small value  $T_{\min} (\approx 0)$ , and minimizes the auxiliary cost  $\mathcal{F}(Z)$  at each  $T$  to obtain

$$Z^* = P^{*t} \Pi, \quad \text{where } Z^* = [z^*(1), \dots, z^*(M)]^t, \quad (10)$$

$$[P^*]_{ij} = \frac{p_i p_{j|i}}{\sum_l p_l p_{j|l}}, \quad p_{j|i} = \frac{\exp\{-(1/T)d(x_i, y_j)\}}{\sum_k \exp\{-(1/T)d(x_i, y_k)\}}, \quad (11)$$

where it utilizes the solution from previous  $T$  iteration to initialize the current iteration.

Note that at large values of  $T$  the weights  $\{p_{j|i}\}$  in (11) are uniformly distributed ( $p_{j|i} = 1/M$ ) and all the representative

distributions  $\{z^*(j)\}$  in (10) are *co-incident*, i.e., effectively  $M = 1$ . It is also known from the sensitivity analysis [13] of the Lagrangian  $\mathcal{L}$  that a large (small)  $T$  corresponds to large (small)  $d_0$  value in (8), and vice-versa. Thus, we infer that large values of  $d_0$  in (8) results into a single distinct representative distribution in  $\{z^*(j)\}$ . With regards to aggregation this means that at large  $d_0$  all the states in  $X$  are well represented by a single super-state. As  $T$  (or, equivalently  $d_0$ ) decreases further the association weights  $\{p_{j|i}\}$  are no longer uniform, and the coincident representative distributions in  $\{z^*(j)\}$  split into distinct groups; thus, the number of distinct distributions in  $\{z^*(j)\}$  increases.

Insights from the simulations of the algorithm in [9] demonstrate that there exist certain critical temperature  $T = T_{cr}$  values at which the solution undergoes *phase transition* characterized by the increase in the number of distinct representative distributions in  $\{z^*(j)\}$ ; where the latter remains unchanged between two consecutive critical temperatures (similar to the MEP-based Deterministic Annealing algorithm [14]). In particular, these critical temperature values  $T_{cr}$ 's occur when the Hessian  $\mathcal{H}(Z^*, P^*, \Psi, T) :=$

$$\left. \frac{\partial^2 \mathcal{F}(Z^* + \epsilon \Psi)}{\partial \epsilon^2} \right|_{\epsilon=0} = \sum_{j=1}^M q_j \psi(j)^T (\Lambda_T(j) - \frac{1}{T} C_T(j)) \psi(j) + T \sum_{i=1}^N \left( \sum_{j=1}^M p_{j|i} \left[ \frac{\pi(i)}{z^*(j)} \right]^t \psi(j) \right)^2, \quad (12)$$

is no longer positive definite. Here  $q_j = \sum_{i=1}^N p_i p_{j|i}$ ,  $\Psi = [\psi(1), \dots, \psi(M)]^t \in \mathbb{R}^{M \times N}$  is the perturbation matrix,

$$\Lambda_T(j) = \text{diag} \left\{ \frac{\sum_{i=1}^N p_{i|j} \pi(i)}{z^*(j)^2} \right\}, \quad (13)$$

$$C_T(j) = \sum_{i=1}^N p_{i|j} \left[ \frac{\pi(i) - z^*(j)}{z^*(j)} \right] \left[ \frac{\pi(i) - z^*(j)}{z^*(j)} \right]^t,$$

and  $p_{i|j} = (p_i p_{j|i} / \sum_l p_l p_{j|l})$  is the posterior distribution.

**Lemma 1.** The Hessian  $\mathcal{H}(Z^*, P^*, \Psi, T)$  in (12) corresponding to the free-energy function  $\mathcal{F}(Z)$  in (9) loses rank when

$$\det[\Lambda_T(j) - \frac{1}{T} C_T(j)] = 0, \quad \text{for some } j \in \{1, \dots, M\}. \quad (14)$$

*Proof.* Please refer to [9].  $\square$

Our current work explicitly derives the critical temperature  $T = T_{cr}^M$  at which the above condition (14) is met as illustrated in the following theorem.

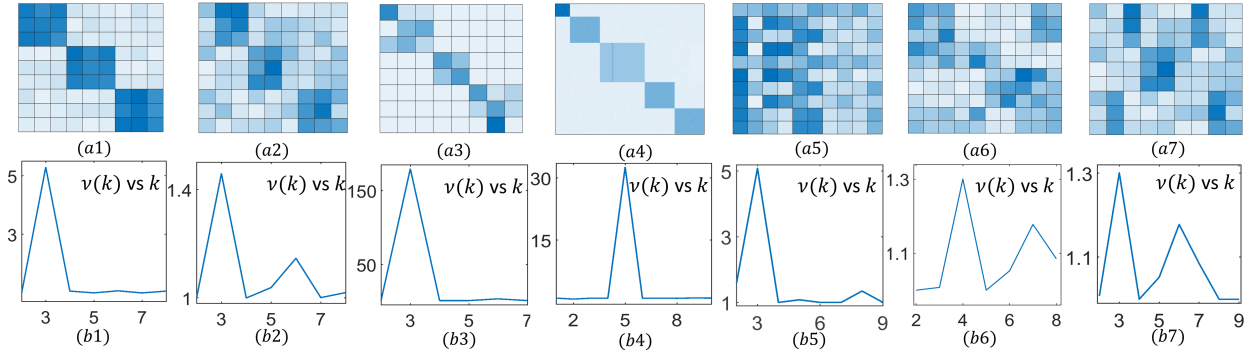


Fig. 3: Illustrates the efficacy of Algorithm 1 in estimating  $k_t$ . (a1)-(a4) demonstrate the heatmaps for the transition matrices of NCD Markov chains generated such that  $N = 9$ ,  $k_t = 3$  in (a1)-(a2),  $N = 8$ ,  $k_t = 3$  in (a3), and  $N = 100$ ,  $k_t = 5$  in (a4). (b1)-(b4) are the corresponding persistence plots that clearly indicate  $v(k_t) > v(k) \forall k \neq k_t$ . (a5)-(a7) illustrate Markov chains generated by considering multiple copies of random vectors  $\{\xi_i \in \mathbb{R}^N\}_{i=1}^{k_t}$ ; where  $N = 10$ ,  $k_t = 3$  in (a5),  $N = 10$ ,  $k_t = 4$  in (a6), and  $N = 9$ ,  $k_t = 3$  in (a7). (b5)-b(7) are the corresponding persistence plot that accurately estimate  $k_t$ .

**Theorem 1.** The critical temperature  $T_{cr}^M$  at which the matrix  $\Lambda_T(j) - \frac{1}{T} C_T(j)$  in (14) is no longer positive definite, and  $Z^*$  in (10) undergoes phase transition is given by

$$T_{cr}^k(Z^*, P^*) := \max_{1 \leq j \leq M} \left[ \lambda_{\max}(\Theta^T C_T(j) \Theta) \right], \quad (15)$$

where  $\lambda_{\max}(\cdot)$  denotes the largest eigenvalue,  $\Theta \in \mathbb{R}^{N \times N-1}$  is as illustrated in Appendix I.

*Proof.* Please refer to the Appendix I.  $\square$

As stated earlier, our expression for the error covariance matrix  $C_X^\Phi(y_j)$  in (1) is motivated from the *soft* covariance matrix  $\Delta(j) := \Theta^T C_T(j) \Theta$  in (15); where the phrase *soft* captures the dependence of  $C_T(j)$  on the association weights  $\{p_{ji}\}$ . More precisely, our expression of the error covariance matrix  $C_X^\Phi(y_j)$  is obtained by substituting  $\{p_{ji}\}$  and  $\{z^*(j)\}$  in  $\Delta(j)$  with the hard-associations as determined by the partition  $\Phi$  and  $\{z(j)\}$  corresponding to the aggregated chain. The largest eigenvalue  $T_{cr}^k$  in (15) captures the spread in representation error (2) in the solution characterized by the soft associations  $\{p_{ji}\}$  and  $\{z^*(j)\}$ . Analogously, the largest eigenvalue  $\bar{T}_k$  of the error covariance matrices captures the spread in the representation error (2) in the solution characterized by the partition function  $\Phi$  and  $\{z^*(j)\}$ .

#### IV. SIMULATIONS

In this section we demonstrate the efficacy of persistence in comparing different aggregated models, and estimating true number  $k_t$  of super-states underlying a Markov chain. We use the Algorithm 1 presented in the Section I that takes the aggregated models at different number  $k$  of super-states as input and outputs the corresponding persistence<sup>2</sup>.

**NCD Markov Chains:** Here, the state transition matrix  $\Pi$  for NCD Markov chains [15] presumes the following structure  $\Pi = \Pi^* + \varepsilon C$ , where  $\Pi^*$  is a block diagonal matrix and  $C$  adds a perturbation of the range  $\varepsilon$ . Naturally, the number  $k_t$  of super-states for such Markov chains can be

approximated to be the number of dominant block diagonals in  $\Pi^*$ . Figures 3(a1)-a(2) illustrate the heatmaps of the transition probability matrix for two NCD chains obtained at different level of perturbations to a three block diagonal matrix  $\Pi^*$ . Figures 3(b1)-(b2) illustrate the persistence  $v(k)$  versus  $k$  plots corresponding to the above Markov chains which correctly identifies the true number  $k_t = 3$  of super-states in both cases. Note that, even though the transition matrix  $\Pi$  in Figure 3(a2) is highly perturbed our method accurately identifies true number of super-states thereby, demonstrating the robustness of persistence  $v(k)$ .

Figure 3(a3) illustrates a specialized NCD Markov chain with Courtois Transition Matrices that are well studied in literature for their slow convergence to the steady state [16]. As is evident from the heatmap, the corresponding Markov chain comprises of  $k_t = 3$  number of super-states which is also captured by our persistence plot in the Figure 3(b3). Figure 3(a4) demonstrates the state transition matrix of a large ( $N = 100$  states) NCD Markov chain, considered in [17], constituting 5 underlying block diagonals (one each of size  $10 \times 10$  and  $30 \times 30$ , and three of size  $20 \times 20$ ). Figure 3(b4) confirms largest persistence at  $k = 5$  number of super-states, and thus, appropriately estimates  $k_t$ .

Further, under additional constraints such as on the maximum dissimilarity permitted ( $c_0 \leq D \leq c_1$ ) between the original and aggregated chains, where  $k_t$  super-states do not satisfy the constraint, we utilize persistence plot to determine the next best choice for the size of the aggregated model. For instance, Figure 3(b2) indicates that  $k = 6$  is the second most persistent number of super-states in the Figure 3(a2) and thus, estimates the appropriate size of the aggregated chain when models with the  $k \leq 3$  are not permitted.

**Randomly generated Markov Chains:** In the following simulations we consider  $N$  state Markov chains where the transition matrices  $\Pi = [\xi_1, \dots, \xi_N]^T + \varepsilon C$  are generated from  $k_t$  random distribution vectors  $\{\xi_i\}_{i=1}^{k_t}$ , and  $\varepsilon C$  introduces perturbations. Naturally,  $k_t$  estimates true number of super-states underlying the above Markov chains. Figure 3(a5)

<sup>2</sup>In our simulations we use the algorithm presented in [9] to determine the aggregated models of a given Markov chain at different values of  $k$ .



illustrates one such scenario where  $\Pi \in \mathbb{R}^{10 \times 10}$  is generated by perturbing multiple copies of  $\{\xi_i\}_{i=1}^3$ , and the persistence plot in Figure 3(b5) accurately determines  $k_t = 3$  as the estimate for the true number of super-states. Similarly, Figures 3(a6) and 3(a7) illustrate the transition matrices  $\Pi \in \mathbb{R}^{10 \times 10}$  generated from 4 and 3 random distribution vectors, respectively, and the persistence plots in Figure 3(b6) and 3(b7) accurately estimate the underlying true number of super-states. Note that even though the perturbations are significantly large in Figures 3(a5)-(a7) persistence  $v(k)$  accurately estimates the number  $k_t$  of super-states.

## V. ANALYSIS AND DISCUSSION

1) *Relation to Data Clustering Problem:* The problem of estimating the true number of super-states in a Markov chain is related to determining the number of clusters in a given data-set. Several works in literature [18]–[22] propose heuristics to estimate the underlying number of clusters, and substantiate their performance through simulations. In particular, it is difficult to provide theoretical guarantees owing to the inherent complexities (such as NP-hardness, and combinatorial decision space) for such problems unless the class of problems are sufficiently constricted; for instance, well-separated spherical clusters, or in our case completely decomposable (CD) Markov chains. The robustness of persistence and our proposed methodology to estimate the true number of super-states is also substantiated by a related work [18] in data clustering that uses a similar methodology as in our work, however, with a different cost function (squared-euclidean distance) and covariance matrix. The proposed methodology in [18] outperforms popular benchmark methods such as gap-statistics [19], X-means [20], G-means and PG-means [21], and dip-means [22] in literature in accurately estimating the number of underlying clusters.

2) *Similar Optimization Problems:* Our framework extends to several other model-reduction techniques such as graph aggregation [17], and co-clustering [23] that pose similar optimization problem as in (7) of aggregating a given matrix  $\mathcal{X} \in \mathbb{R}^{N_1 \times N_2}$  to a smaller representative matrix  $\mathcal{Y} \in \mathbb{R}^{M_1 \times M_2}$ ; where, the size of the reduced model is not known a priori and thus, needs to be estimated. These method find application in areas such as text mining, image segmentation, and collaborative filtering [23].

## APPENDIX I

$\theta = \Phi G$  where  $\Phi = [I_{N-1 \times N-1} \ 0_{N-1}]^T + (-\frac{1}{N} \mathbf{1}_{N \times N-1})$ ,  $G = L_\Delta^{-1} P_\Delta$  where  $L_\Delta$  is Cholesky decomposition of  $\Phi^T \Lambda_T(j) \Phi$  and columns of  $P_\Delta$  are the eigenvectors of  $L_\Delta^{-1} [\Phi^T C_T(j) \Phi] L_\Delta^{-1}$ .  $\Lambda_T(j)$ ,  $C_T(j)$  in (13).

**Proof of Theorem 1:**  $\Psi_j = \bar{\Phi} K_j \in \mathbb{R}^N$  where  $\bar{\Phi} \mathbf{1}_N = 0$  for admissible perturbations [9],  $\text{rank}(\bar{\Phi}) = N - 1$ , Let  $\bar{\Phi} \in \mathbb{R}^{N \times N-1}$  with  $\text{Range}(\bar{\Phi}) = \text{Range}(\Phi)$ . Let  $\bar{K}_j \in \mathbb{R}^{N-1}$  such that  $\bar{\Phi} K_j = \Phi \bar{K}_j$ , then  $\psi_j = \Phi \bar{K}_j$ . By (14)  $\exists \psi_j \in \mathbb{R}^N$  such that  $\psi_j^T (\Lambda_T(j) - \frac{1}{T} C_T(j)) \psi_j = 0$  implies  $\bar{K}_j^T (\Phi^T \Lambda_T(j) \Phi - \frac{1}{T} \Phi^T C_T(j) \Phi) K_j = 0$ . From Theorem 12.19 in [24]  $\exists G \in \mathbb{R}^{N-1 \times N-1}$  such that  $G^T H_0 G = I$  and  $G^T H_1 G = \Delta$  where  $G = L_\Delta^{-1} P_\Delta$ ,  $H_0 = L_\Delta L_\Delta^T$ ;  $P_\Delta$  is such that  $P_\Delta^T [L_\Delta^{-1} H_1 L_\Delta^{-1}] P_\Delta = \Delta$ .

Let  $\bar{K}_j = G \omega_j$ ,  $\omega_j \in \mathbb{R}^{N-1}$ ,  $\omega_j^T (G^T H_0 G - \frac{1}{T} G^T H_1 G) \omega_j = 0 \implies \det(I - \frac{1}{T} \Delta) = 0 \implies T = \lambda_{\max}(\Delta)$ .

## REFERENCES

- [1] P. A. Gagniuc, *Markov chains: from theory to implementation and experimentation*. John Wiley & Sons, 2017.
- [2] R. Srikant, *The mathematics of Internet congestion control*. Springer Science & Business Media, 2004.
- [3] C. J. Quinn, T. P. Coleman, N. Kiyavash, and N. G. Hatsopoulos, "Estimating the directed information to infer causal relationships in ensemble neural spike train recordings," *Journal of computational neuroscience*, vol. 30, no. 1, pp. 17–44, 2011.
- [4] H. A. Simon and A. Ando, "Aggregation of variables in dynamic systems," *Econometrica: journal of the Econometric Society*, pp. 111–138, 1961.
- [5] R. W. Aldhaheri and H. K. Khalil, "Aggregation of the policy iteration method for nearly completely decomposable markov chains," *IEEE Transactions on Automatic Control*, vol. 36, no. 2, pp. 178–187, 1991.
- [6] M. Vidyasagar, "A metric between probability distributions on finite sets of different cardinalities and applications to order reduction," *IEEE Transactions on Automatic Control*, vol. 57, no. 10, pp. 2464–2477, 2012.
- [7] Y. Xu, S. M. Salapaka, and C. L. Beck, "A distance metric between directed weighted graphs," in *52nd IEEE Conference on Decision and Control*. IEEE, 2013, pp. 6359–6364.
- [8] K. Deng, P. G. Mehta, and S. P. Meyn, "Optimal kullback-leibler aggregation via spectral theory of markov chains," *IEEE Transactions on Automatic Control*, vol. 56, no. 12, pp. 2793–2808, 2011.
- [9] Y. Xu, S. M. Salapaka, and C. L. Beck, "Aggregation of graph models and markov chains by deterministic annealing," *IEEE Transactions on Automatic Control*, vol. 59, no. 10, pp. 2807–2812, 2014.
- [10] K. Chaudhuri and A. McGregor, "Finding metric structure in information theoretic clustering," in *COLT*, vol. 8. Citeseer, 2008, p. 10.
- [11] I. J. Sledge and J. C. Pri'ncipe, "An information-theoretic approach for automatically determining the number of state groups when aggregating markov chains," in *ICASSP 2019-2019 IEEE International Conference on Acoustics, Speech and Signal Processing (ICASSP)*. IEEE, 2019, pp. 3612–3616.
- [12] T. M. Cover, *Elements of information theory*. John Wiley & Sons, 1999.
- [13] E. T. Jaynes, *Probability theory: The logic of science*. Cambridge university press, 2003.
- [14] K. Rose, "Deterministic annealing, clustering, and optimization," Ph.D. dissertation, California Institute of Technology, 1991.
- [15] A. Ando and F. M. Fisher, "Near-decomposability, partition and aggregation, and the relevance of stability discussions," *International Economic Review*, vol. 4, no. 1, pp. 53–67, 1963.
- [16] A. L. Elsayad, "Numerical solution of markov chains," 2002.
- [17] Y. Xu, "Clustering, coverage and aggregation methods for large networks," Ph.D. dissertation, University of Illinois at Urbana-Champaign, 2015.
- [18] A. Srivastava, M. Baranwal, and S. Salapaka, "On the persistence of clustering solutions and true number of clusters in a dataset," in *Proceedings of the AAAI Conference on Artificial Intelligence*, vol. 33, 2019, pp. 5000–5007.
- [19] R. Tibshirani, G. Walther, and T. Hastie, "Estimating the number of clusters in a data set via the gap statistic," *Journal of the Royal Statistical Society: Series B (Statistical Methodology)*, vol. 63, no. 2, pp. 411–423, 2001.
- [20] D. Pelleg, A. W. Moore, et al., "X-means: Extending k-means with efficient estimation of the number of clusters," in *Icml*, vol. 1, 2000, pp. 727–734.
- [21] Z. Feng, R. Dearden, N. Meuleau, and R. Washington, "Dynamic programming for structured continuous markov decision problems," in *Proceedings of the 20th conference on Uncertainty in artificial intelligence*. AUAI Press, 2004, pp. 154–161.
- [22] A. Kalogeratos and A. Likas, "Dip-means: an incremental clustering method for estimating the number of clusters," in *Advances in neural information processing systems*, 2012, pp. 2393–2401.
- [23] I. S. Dhillon, S. Mallela, and D. S. Modha, "Information-theoretic co-clustering," in *Proceedings of the ninth ACM SIGKDD international conference on Knowledge discovery and data mining*, 2003, pp. 89–98.
- [24] A. J. Laub, *Matrix analysis for scientists and engineers*. Siam, 2005, vol. 91.